Scale effects on ship vertical force and trim moment in calm water

Maxime Le Strat ⊙ ; Momchil Terziev ✉ ⊙

Check for updates

View Online

Export Citation

Articles You May Be Interested In

Propeller–hull interaction simulation for self-propulsion with sinkage and trim

Physics of Fluids (February 2024)

Calm water resistance prediction of a bulk carrier using Reynolds averaged Navier-Stokes based solver

AIP Conference Proceedings (December 2017)

Study of middle interceptor implementation on patrol boat

AIP Conf. Proc. (May 2023)

Scale effects on ship vertical force and trim moment in calm water

View Online   Export Citation   CrossMark

Maxime Le Strat[1,2] (iD) and Momchil Terziev[1,a)] (iD)

AFFILIATIONS

[1]Department of Naval Architecture, Ocean and Marine Engineering, University of Strathclyde, Glasgow, United Kingdom
[2]Department of Mechanical Engineering (DGM), Ecole Normale Supérieure de Paris-Saclay, Gif-sur-Yvette, France

[a)]Author to whom correspondence should be addressed: momchil.terziev@strath.ac.uk

ABSTRACT

Predicting ship resistance with high accuracy is essential to reduce fuel consumption. Of the two currently available methods, extrapolation from models-scale using towing tank results shows high levels of uncertainty, and while computational fluid dynamics is a promising option to reduce this uncertainty, recent full-scale simulations show persistently high errors. Another way to reduce the uncertainty is to understand the scale effects and devise strategies to account of them. In this paper, we explore the scale effects on ship trim and sinkage through numerical simulations using viscous and linear scaling with three different turbulence models. We demonstrate that the scale effect on sinkage can be neglected. However, between $Re = 10^6$ and $Re = 10^8$, depending on the turbulence model, scale effects on the trim moment range from 15% to 27%, and differences in pressure coefficient on the hull can be observed between the different Reynolds numbers, especially around the aft of the ship of between 23.6% and 32.5%.

I. INTRODUCTION

To design ship hulls, naval architects require an accurate estimate of the total resistance of the ship at full-scale. Historically, naval architects have measured the resistance at models-scale in towing tanks and extrapolated to full-scale. However, extrapolation methods are limited by assumptions and neglect of scale effects acting on the constituent components of ship resistance. Although full-scale numerical simulations are becoming more accessible, a recent blind workshop on full-scale resistance of a ship showed mixed success in providing accurate predictions (Ponkratov, 2017). Another way to approach the problem is to demonstrate, understand, and ultimately overcome scale effects that presently cause epistemic errors and uncertainties. Therefore, it is important to identify the factors affecting the components of ship resistance, to understand which of these components suffer from scale effects and why.

To measure the resistance of a ship, the ITTC-endorsed approach follows Hughes' form factor, $(1+k)$, dependent solely on the shape of the hull (ITTC, 2017). The total resistance coefficient is then decomposed as $C_T = (1 + k)C_F + C_W$, where C_T, C_F, and C_W are the total, frictional, and wave resistance coefficients, respectively. The form factor is estimated using a Prohaska test, which involves the towing of a ship at very low speeds, where C_w may be neglected (Korkmaz et al.,

2019). Alternatively, computational fluid dynamics (CFD) modeling may be used in double body mode, that is, where the water surface is replaced by a symmetry plane to eliminate C_w. The present study uses that approach to eliminate the wave resistance.

Each component of the total resistance is associated with a unique set of challenges and methods that aim to address these. Scale effects, that is, variation with Reynolds number of parameters that are theoretically independent of viscous effects, such as the wave resistance and form factor, are a key barrier to reliable extrapolation. Nevertheless, these scale effects are documented, and approaches to correct for them are available (García-Gómez, 2000; Min and Kang, 2010). While it is known that sinkage and trim affect resistance, the scale effect on the running sinkage and trim of a ship and how these affect the other properties are rarely studied in the literature. For example, a trim optimization study may recommend a small trim by bow to reduce the overall resistance, but virtually no contemporary evidence exists to definitively rule out, or otherwise, the influence of Reynolds number effects on parameters such as sinkage and trim is thought to depend on the Froude number only. Trim optimization, a widely used method to improve the energy efficiency of a ship without any alteration to the ship structure or retrofitting, may, therefore, be questionable if conducted at the model scale.

The present paper provides evidence of the existence of scale effects on the running trim and sinkage of a ship through the use of Reynolds Averaged Navier–Stokes (RANS) computational fluid dynamics. We make use of boundary layer physics to explain why such a scale effect should exist using first principles. Double body numerical simulations are used to control all parameters affecting the resistance of a ship, thus eliminating the possibility of the observed results being contaminated by secondary effects. In addition, the definition of the form factor is reexamined with the aim of reducing the impact of its scale effects on the predictive accuracy of full-scale ship resistance.

The remainder of the paper is organized as follows. Section II lays out the pertinent background and explains the historical and recent contributions to the study of scale effects with a focus on the form factor, sinkage, and trim. Section III specifies the case studies and conditions employed along with the properties of the numerical environment. This is followed by an explanation of the numerical modeling in Sec. IV, which precedes the results and discussions in Sec. V. Finally, Sec. VI highlights the conclusions and sets out future research directions.

II. BACKGROUND

The dependence of the form factor on the Reynolds number ($Re = VL\rho/\mu$, where V is the ship speed, L is the ship length, ρ is the water density, and μ is the dynamic viscosity of water) is well-known from experimental and numerical studies such as García-Gómez (2000) and Terziev et al. (2019), and evidence to suggest a dependence on the Froude number also exists (Terziev et al., 2021a). However, according to Yokoo (1960), "*the cause for the variation of form factor, however, is not Froude number or ship's speed itself, but change of trim and sinkage of a ship due to change of ship's speed.*" Abundant evidence from computational fluid dynamics-derived solutions shows that the form factor varies even when the ship sinkage and trim are fixed (Korkmaz et al., 2021); therefore, Yokoo's (1960) assertion cannot represent the full picture. Nevertheless, Yokoo's (1960) hypothesis has not yet been definitively proven or disproven. Nor is the magnitude of the scale effect demonstrated, if it exists.

Since it is postulated by Yokoo (1960) that the form factor scale effects are solely due to changes in sinkage and trim, it is instructive to examine the approaches to calculating the form factor. In the literature, two definitions of the form factor can be found:

(1) $(1 + k) = C_T/C_{F, ITTC}$, that is, the ratio between the total resistance and the frictional resistance obtained through the ITTC correlation line. This is the standard definition adopted by the ITTC.
(2) $(1 + k) = C_V/C_{F, CFD}$, that is, the ratio of the viscous and frictional resistances, both of which can be obtained through CFD. This is not an accepted definition despite its similarity to Eq. (1).

Regardless their apparent disagreements, both definitions suffer from the same problem. They are in direct contravention to the formal definition of the form factor. That is, neither definition uses a flat plate friction line: $(1 + k)$ is defined as the ratio of the ship's total resistance in the absence of waves, and the frictional resistance of a flat plate of equivalent surface area. As all relevant ITTC documents point out, the ITTC57 line is a correlation line and not a flat plate line. Even if the original definition of the form factor with reference to a flat plate

friction line were to be strictly adhered to, there is no agreement on which equation represents the friction of a flat plate, particularly at high Reynolds number in the region 10^8–10^9 where most commercial ships operate.

CFD-based form factors were recently investigated by Korkmaz et al. (2021). They concluded that "*CFD based form factors can be considered as an alternative or supplementary method to the Prohaska method.*" Similarly, Wang et al. (2019) made the same conclusion as Korkmaz et al. (2021), showing that the CFD/EFD combination method would be promising in alleviating scale effects by increasing the accuracy in form factor predictions, especially for ships with bulbs or large transoms. These approaches retain their reliance on friction lines, which, in many cases, must be derived in-house based on an analyst's experience and preference. Thus, reliance on custom friction lines cannot solve the problem of scale effects since their slope, particularly at high Reynolds numbers, is associated with high levels of uncertainty.

Yokoo (1960) supposed that the form factor's apparent dependence on the Froude number is a secondary effect caused by trim and sinkage. He showed a dependency of the trim angle on F_n, particularly for small F_n, explaining the change in form factor could be due to changes in the trim angle, sinkage, and wetted area with a F_n change. It may be postulated that uncertainties in measurement of small trim and sinkage at very low speeds may be responsible for Yokoo's (1960) observations. More recently, Terziev et al. (2021a) confirmed that past a certain speed range, the form factor is essentially F_n-independent using computational fluid dynamics modeling.

It is well-known that sinkage, trim, and resistance are dependent on the forward speed. However, Ferguson (1977) asserted that changes in sinkage and trim are significant factors in resistance extrapolation because they modify the shape of the underwater hull. According to Ferguson (1977) and as demonstrated by a number of studies, even when the sinkage and trim are fixed, the variation in the form factor due to Re is still observed (Terziev et al., 2021a).

Due to a lack of experimental data at full scale and the large measurement uncertainties in the model scale (Elsherbiny et al., 2019), the examination of scale effects on trim and sinkage has not been studied extensively, and conflicting information in the literature regarding the existence of such scale effects exists. For example, Gourlay and Tuck (2001) argued that a viscous effect on trim likely exists due to possible flow separation at the stern. More recently, computational work by Kok et al. (2020) claimed that scale effects on sinkage and trim do not exist. However, a reexamination of their results shows that sinkage changed by 5.32% at the relatively low speed (and therefore, Reynolds number) corresponding to 13.3 kn.

Recent full-scale simulations showed that there is some way to go before results can become reliable for routine analysis. For instance, in the first ship-scale hydrodynamics workshop (Ponkratov, 2017), the difference between the highest and the lowest resistance was around 15% depending on velocity. The same workshop showed similar results for sinkage, but trim was considerably more difficult to predict for participants showing differences of approximately a factor of 6 in some cases between predictions and measurements. Blind application of ever-increasing cell numbers is therefore not likely to yield improvements in accuracy, as summarized by Terziev et al., (2022), and in the meantime, it is important to better understand scale effects since they influence resistance extrapolation.

TABLE I. Principal characteristics of the KCS ship.

Quantity	Symbol	Model-scale	Full-scale	Unit
Scale factor	λ	31.599	1	$\cdots$
Length	L	7.279	230	m
Beam	B	1.019	32.2	m
Depth	D	0.601	19	m
Draught	T	0.342	10.8	m
Displacement	∇	1.649	52028	m^3
Block coefficient	C_B	0.651	0.651	$\cdots$
Wetted area with rudder	S_w	9.553	9538	m^2

Despite the advent of high-resolution numerical models, advanced experimentation techniques, and decades of research, the question of whether scale effects act on the vertical attitude of a ship in calm water has not been answered with certainty. We argue that scale effects must have some contribution to a ship's dynamic attitude in calm water due to the nature of boundary layers. The magnitude of such changes, however, is not known and likely depends on the shape of the hull. As discussed in detail by Gourlay and Tuck (2001), the varying thickness of the boundary layer and velocity distribution therein will cause some changes in the pressure at the stern at full-scale relative to model-scale. Transom sterns where separation-induced changes are important are more likely to have a stronger scale effect relative to non-transom sterns.

III. CASE STUDIES

The KRISO container ship (KCS) is used throughout the present study at the operational Froude number of $F_n = 0.26$, equivalent to 24 knots (Kim *et al.*, 2001). The principal characteristics of the KCS are given in Table I. The Froude number is fixed in all instances to ensure that subsequently obtained results are not subject to variation from

FIG. 1. Form factor predictions against Reynolds number for the KCS. Dataset obtained from Terziev *et al.* (2021a) and updated to include their results.

dimensionless groups other than the Reynolds number, which is systematically varied. Making use of the KCS also allows the present study to compare form factor estimates across multiple Reynolds numbers derived experimentally and numerically. For example, Terziev *et al.* (2021a) compiled a dataset of such studies, which is reproduced here with the addition of a sample of the results obtained by Terziev *et al.* (2021a), as shown in Fig. 1.

According to Fig. 1, the form factor of the KCS generally increases with Reynolds number although there is a significant amount of scatter in both experimental and numerical data. The approach taken in the present paper is to first compare a result that is directly comparable to available experiments in terms of scale factor. Specifically, the scale factor of $\lambda = 31.599$ is chosen as it produces the model with the largest length. Subsequently, Reynolds numbers 10^6, 5×10^6, 10^7, 5×10^7, and 10^8 are modeled while maintaining the ship length but altering the viscosity of the water. This is a useful approach to model ship resistance at varying Reynolds number (Haase *et al.*, 2016). To ensure the validity of results obtained by varying the viscosity of water, an additional set of numerical simulations are carried out where the ship is physically scaled to match the same Reynolds numbers (10^6, 5×10^6, 10^7, 5×10^7, and 10^8) for a fixed Froude number ($F_n = 0.26$). The resulting test matrix is given in Table II.

IV. NUMERICAL MODELING

The commercially available finite volume solver, Star-CCM+, version 17.04.008 with double precision, was used throughout. The automatic meshing facilities within the solver were employed to create unstructured hexahedral grids on which to solve the Reynolds Averaged Navier–Stokes equations. As discussed previously, employing the double body allows all simulations to be run in steady state. In addition, ship vertical motions, that is, sinkage and trim, are not modeled. Neglecting the full set of physical phenomena acting on the ship, specifically, the free surface, is associated with inherent limitations. The total resistance coefficient cannot be estimated since the wave resistance is excluded. The variation in the free surface profile on the hull surface also cannot be captured. The scale effect on this component is thought to be small, making this a valid assumption.

As shown in Sec. II, sinkage and trim modeling and measurement suffer from considerable uncertainties. The present paper, therefore, measures the force and moment causing the sinkage and trim, which
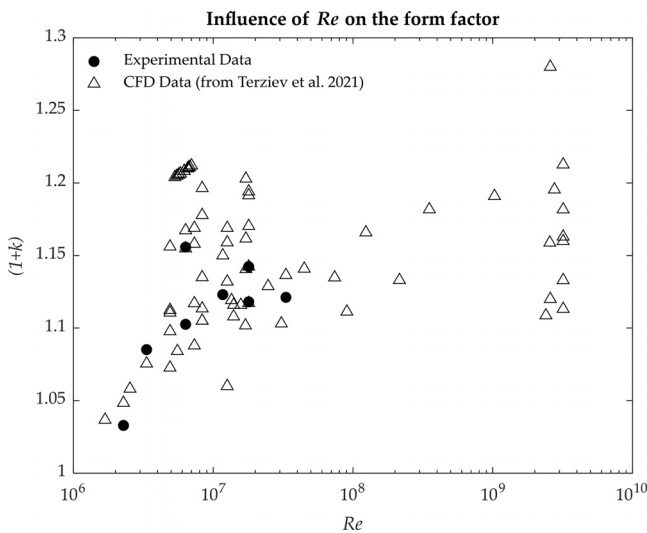
TABLE II. Case studies modeled using linear and viscous scaling.

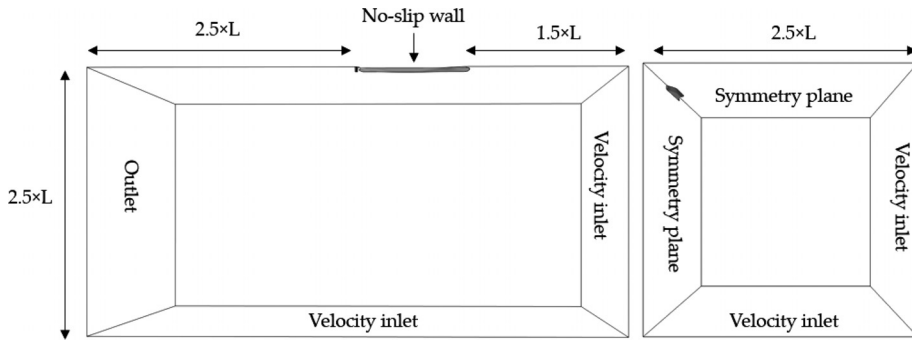| Case number	Re	Viscosity (Pa-s)	Scale factor	V_∞ (m/s)	Fr
1	10^6	8.8875×10^{-4}	216	0.84	
2		1.59×10^{-2}	31.599	2.197	
3	5×10^6	8.8875×10^{-4}	74.2	1.434	
4		3.2×10^{-3}	31.599	2.197	
5	10^7	8.8875×10^{-4}	46.6	1.809	
6		1.6×10^{-3}	31.599	2.197	0.26
7	5×10^7	8.8875×10^{-4}	16	3.088	
8		3.19×10^{-4}	31.599	2.197	
9	10^8	8.8875×10^{-4}	10	3.905	
10		1.6×10^{-4}	31.599	2.197	

FIG. 2. Computational domain dimensions and boundary conditions.

can be predicted with less uncertainty. For simplicity, it is assumed that the ship sinks and trims around its center of gravity. All discretization orders are set to second order accuracy.

A. Computational domain

The computational domain consists of a rectangular box with dimensions set in multiples of the ship length. In the x direction, the domain inlet is set around 1.5 ship length upstream of the forward perpendicular where the fluid velocity is introduced, while the outlet is placed around 2.5 ship lengths downstream of the aft perpendicular where a pressure outlet maintains 0 pressure. A 0-pressure condition is admissible since in the double body mode, gravity is not relevant and therefore not modeled, making the pressure equivalent to the dynamic pressure. The domain side and bottom are placed 2.5 ship lengths from the ship centerline where symmetry plane and velocity inlet conditions are implemented, respectively. The velocity inlet is a Dirichlet type boundary condition, which is used to introduce the uniform flow in the domain in the negative x-direction only, thus mimicking the forward motion of the vessel. Finally, the domain top is placed to match the design draft of the ship. This boundary along with a plane bisecting the ship is symmetries. These boundary conditions are summarized in Fig. 2.

B. Near-wall mesh

An accurate representation of the resistance of the ship is highly sensitive to near-wall meshing, particularly in double body mode where friction accounts for a vast majority of the total. To ensure consistent results, the methodology given in Terziev *et al.* (2022) to construct the mesh is employed. The procedure begins with an estimate of the frictional resistance of the ship through the ITTC correlation line,

$$C_F = \frac{0.075}{\left(\log_{10}(Re) - 2\right)^2}. \tag{1}$$

Once the frictional resistance coefficient is known, it is possible to obtain the local shear stress, τ_w, as shown in the following equation:

$$\tau_w = C_F \rho V^2 / 2. \tag{2}$$

By using a geometric series along with the first cell height, $2dy$, as shown in Eq. (3), it is possible to fully define the distribution of cells within the boundary layer, as shown in Eq. (4). The first 20%

of the boundary layer (δ_{20}) is discretized in this way by assuming that the ship's boundary layer is of the same thickness as that of a flat plate with the same Reynolds number, as shown in Eq. (5),

$$dy = y^+ \nu / \sqrt{\tau_w / \rho}, \tag{3}$$

$$n = \log\left(1 - \frac{\delta_{20}(1 - S)}{2dy}\right) \Big/ \log(S), \tag{4}$$

$$\delta_{20} = 20\% \times 0.382 L / Re^{1/5}, \tag{5}$$

where n is the number of layers and $S = 1.2$ is the common ratio of the geometric series, representing the ratio of any two adjacent near-wall layers. By solving Eq. (3) for the target y^+ value, it is possible to set an approximate desired range for the y^+ value to be achieved. In addition, the resolution of the near-field disturbance, or the Bernoulli effect caused by the hull, whereby pressure is reduced and velocity increased, is modeled by allowing cells to double in dimensions in layers of 8 cells. This ensures adequate resolution in the vicinity of the ship. A 3D view of the generated mesh is presented in Fig. 3. The target y^+ value in all case studies was set to 50 to ensure accurate representation of near-wall quantities. The achieved y^+ values across all studies are $y^+ = 50 \pm 5$.
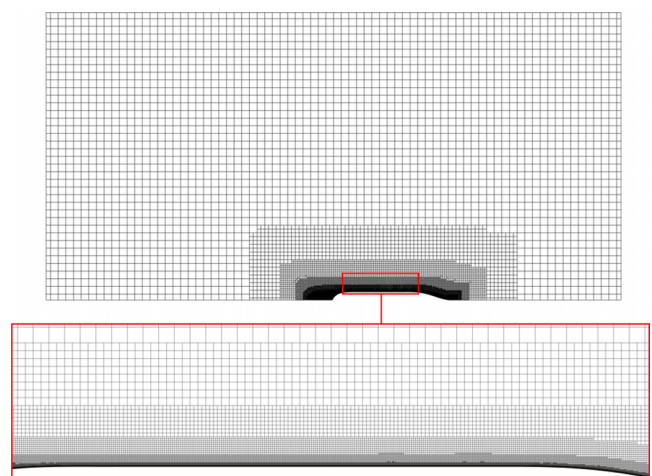

FIG. 3. Top view of the generated mesh. Case depicted: mesh around the hull for $\lambda = 10$ and $Re = 10^8$.

C. Turbulence modeling

Modeling errors, introduced by the choice of turbulence model, are handled by employing three widely used turbulence models: specifically, the realizable $k - \varepsilon$ model, the standard $k - \omega$ model (Wilcox, 2008), and the Shear Stress Transport (SST) model (Menter, 1994). These turbulence models represent the most widely used turbulence models in ship hydrodynamics and are known to provide robust results (Terziev *et al.*, 2020).

V. RESULTS AND DISCUSSION

To ensure data from different scale factors can be compared directly, results must be made dimensionless. In the case of resistance, it is known that the viscous resistance, modeled in the present paper through double body simulations, decreases monotonically. That is a phenomenon primarily driven by the reduction in the value of the frictional resistance coefficient with increasing *Re*. In addition, it is known that the viscous pressure resistance coefficient shows a similar monotonic decrease with scale factor. Thus, the three resistance coefficients are all expected to decrease in value. Their definition follows the standard form: $C_{T,F,VP} = R_{T,F,VP}/(0.5\rho SV^2)$, where the subscripts *T*, *F*, and *VP* indicate the total, frictional, and viscous pressure component, respectively. It should be noted that the viscous resistance is treated as the total for the purposes of the present paper. For simplicity, the vertical force (C_S, subscript S to denote sinkage) is made dimensionless using the same procedure, which is positive upward, while the trimming moment (C_M) is further divided by the length of the ship ($0.5\rho SV^2 L$).

A. Verification study

Mapping the continuous form of the governing partial differential equations onto discrete intervals in space gives rise to error, known as the discretization error. Any solution obtained from a computational fluid dynamics solver must estimate that error and the resulting uncertainty (Roache *et al.*, 1986). The discretization error is typically estimated through a procedure based on Richardson extrapolation (Richardson, 1911; Richardson and Gaunt, 1927), which requires a minimum of two solutions obtained on systematically varied grids. In such a case, the order of accuracy is assumed to match the theoretical order of accuracy, $p_t = 2$. That is, the power dominating the power series decomposition of the error as a function of the fine solution, an unknown exact solution, and the grid spacing. However, two solutions are not thought to be sufficient to capture the behavior of the solution with grid refinement; thus, three systematically refined solutions are used to predict the value of the observed order of accuracy (ITTC,

2008). These solutions are known as the fine, medium, and coarse solutions with reference to the grid dimension. To ensure the validity of the Richardson extrapolation procedure, all cell aspect ratios must remain the same across the so-called grid triplet (Salas, 2006).

The present paper employees the grid convergence index (Roache, 1997) to estimate the uncertainty (*U*). When f_1, f_2, and f_3, the fine, medium, and coarse solutions, respectively, are obtained, and the type of behavior with approach to the asymptotic range is estimated through the refinement factor, *R*:

$$R = \frac{f_2 - f_1}{f_3 - f_2}. \tag{6}$$

When $|R| < 1$, the solution is converging, and if, in addition, $R > 0$, the solution is monotonically converging, whereas if $-1 < R < 0$, the solution is exhibiting oscillatory convergence. On the other hand, if $|R| > 1$, the solution is diverging, or the mode of approach to the asymptotic range cannot be estimated.

The observed order of accuracy, *p*, is then obtained as shown in the following equation:

$$p = \log\left(\frac{f_3 - f_2}{f_2 - f_1}\right) \Big/ \log(r), \tag{7}$$

where $r = \sqrt{2}$ is the refinement ratio as recommended by the American Society of Mechanical Engineers (ASME, 2009), representing the ratio of a cell in any two adjacent refinement steps. The fine, medium, and coarse solutions were obtained using 1 184 153 cells, 683 858 cells, and 395 906 cells, respectively. Once the order of accuracy is obtained, the uncertainty follows:

$$U = 1.25 \left(\frac{f_2 - f_1}{r^p - 1}\right) \Big/ f_1, \tag{8}$$

where the factor of 1.25 is known as the Factor of Safety. This factor magnifies the discretization error to encompass the exact solution with 95% confidence interval. The uncertainty is a symmetrical band around the fine solution and does not have a sign.

The grid convergence index procedure is applied on the two definitions of the form factor, the total resistance, the vertical force due to the pressure drop surrounding the ship, and the trimming moment. Table III shows that the approach to setting up the numerical simulation exhibits solely monotonic convergence across the parameters investigated.

The order of accuracy in all cases is close to the theoretical value. It is well-known that very high observed orders of accuracy artificially reduce the value of uncertainty. This has led to the development of

TABLE III. Results from the verification study.

Parameter	$(1+k)$ (CFD)	$(1+k)$ (ITTC)	C_T	C_s	C_M
f_1	1.084	1.142	3.108×10^{-3}	2.892×10^{-2}	1.212×10^{-3}
f_2	1.088	1.154	3.141×10^{-3}	2.892×10^{-2}	1.205×10^{-3}
f_3	1.095	1.172	3.190×10^{-3}	2.891×10^{-2}	1.193×10^{-3}
R	0.623	0.658	0.658	0.533	0.648
p	1.366	1.209	1.207	1.814	1.254
U (%)	0.78	2.50	0.024	1.39	2.51

methodologies that introduce what are essentially penalty factors for deviation from the theoretical order of accuracy, particularly when $p = 2$ is exceeded (Xing and Stern, 2010). The numerical simulation shows that the parameters of interest do not exceed the theoretical value of 2. In addition, the overall uncertainty is in all cases low. The trimming moment and ITTC-derived form factor show the highest level of uncertainty of 2.5%, which is deemed acceptable. Similarly, the ITTC-based experimentally obtained form factor values depicted in Fig. 1 for a Reynolds number of approximately 1.8×10^6 are approximately 1.42, showing excellent agreement with the value obtained herein.

Typically, the spatial discretization error is but one of the components of the numerical error. The other two key components are errors due to temporal discretization and iterative errors, which magnify other discretization errors (Eca *et al.*, 2017). In the present paper, a steady state model is used, negating the temporal discretization term. The iterative error is minimal in all cases, which is achieved by reducing the magnitude of residuals by at least 4 orders of magnitude. Other types of numerical error, such as the modeling error due to the turbulence closure, are dealt with by accounting for multiple turbulence models, as discussed subsequently. Therefore, the discretization error can be used as a measure for the total numerical error.

B. Ship resistance

The first set of results to be examined pertain to the components of ship resistance. Since double body simulations are used, the chief component of the total is the frictional resistance. To obtain a measure of quality of the solution, the computed frictional resistance coefficients are compared against the ITTC correlation line. Figure 4 shows the performance of the numerical set up has been successful in closely tracking the ITTC correlation line across the examined Reynolds number range.

Modeling differences between the two turbulence models have the effect of a systematic underprediction in the case of the k-ε and SST models. When using the k-ω Wilcox model, on the other hand, the CFD model predicts values that are both lower and higher than the ITTC correlation line depending on the Reynolds number. Since it is known that the ITTC correlation line is a highly accurate surrogate for the KCS' frictional resistance coefficient in the examined Reynolds number range, it can be concluded that superior behavior has been shown by the k-ω Wilcox model. Similar findings in addition to computational efficiency have been reported previously (Terziev *et al.*, 2020).

The aim of the present study is to test if scale effects act on ship trim and sinkage. To avoid pitfalls of previous studies where the potential for such effects was obscured by the presence of other phenomena, such as unsteadiness due to self-propulsion, or uncertainty in measuring ship running sinkage and trim, the present study opted to represent sinkage and trim via a surrogate. Instead of modeling physical sinkage and trim, the vertical force and trimming moment are measured in a double body model.

Applying Buckingham π theorem-type reasoning, one can show that sinkage and trim in dimensionless or coefficient form should not depend on viscosity. Hence, if the force and moment causing sinkage and trim change, then so must sinkage and trim. Since dimensionally consistent parameters are used, if any variation, greater than the discretization uncertainty, is observed, then
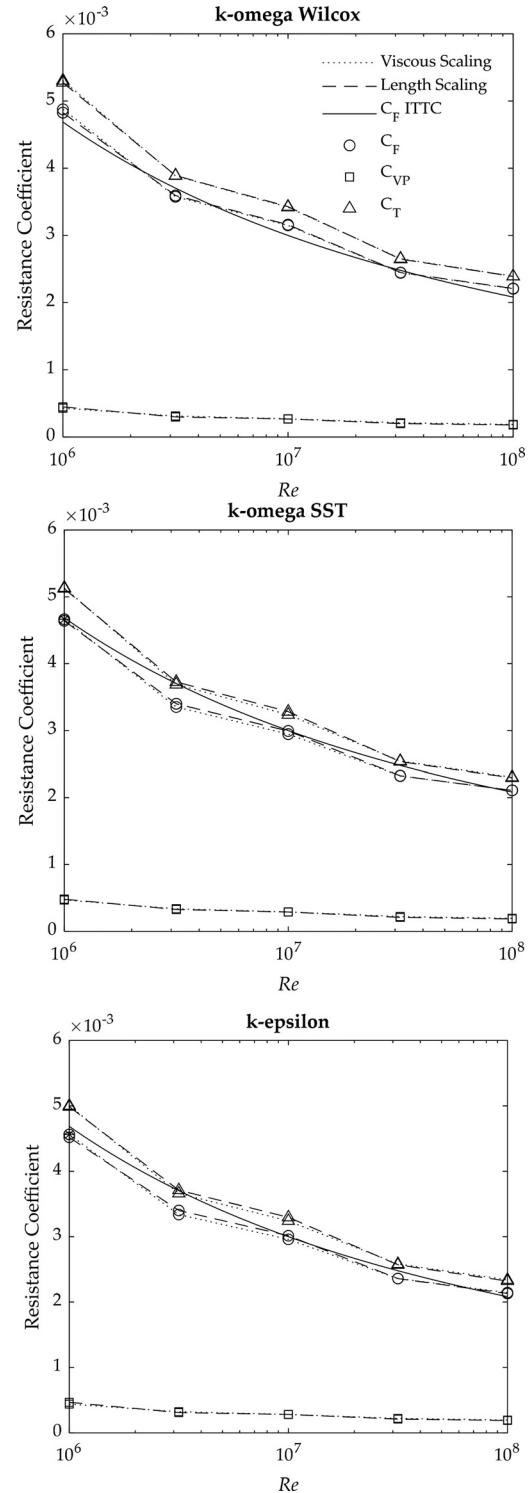
FIG. 4. Resistance coefficients compared with the ITTC correlation line for different turbulence models over the entire range of Reynolds numbers. Dashed lines show linear length scaling, while dotted lines indicate viscous scaling. Reynolds number-dependence of the vertical force and trimming moment.

scale effects can be said to have been demonstrated. In summary, by fixing the trim rotation and the vertical displacement of the ship, it is possible to track the evolution of the trim moment and the vertical force with variable Re and observe the difference (in absolute value and in %) as the Reynolds number increases by two orders of magnitude, between $Re = 10^6$ and $Re = 10^8$.

It should be noted that the approach in studying the properties of sinkage and trim has long been used with good success. For example, the theory developed by Tuck (1966) and its subsequent extensions and modifications (Beck *et al.*, 1975; Gourlay, 2003; and Tuck, 1967) have proven the approach of predicting forces, and moments can be converted into displacement magnitudes with excellent accuracy. Thus, the method employed herein breaks no precedent while successfully isolating and controlling for the properties of interest.

Figure 5 shows the vertical force coefficient values obtained for each case in addition to the relative change from the lowest Reynolds number (10^6). All analysis methods employed show that the sinkage force increases in the absolute value. However, differences are less than 1% between $Re = 10^6$ and $Re = 10^8$, which falls within the discretization uncertainty calculated in Sec. V A. It is, therefore, confirmed that scale effects do not act on sinkage. Figure 5 also depicts that modeling errors, such as those caused by the choice of turbulence model, are more significant at model-scale than they are at full-scale. Such a conclusion may be reached based on larger range of predicted vertical force coefficients at model than at full-scale.

By contrast, Fig. 6 shows that the trim moment coefficient exhibits significant variation in magnitude over the examined Reynolds number range. The largest deviation between $Re = 10^6$ and $Re = 10^8$ is
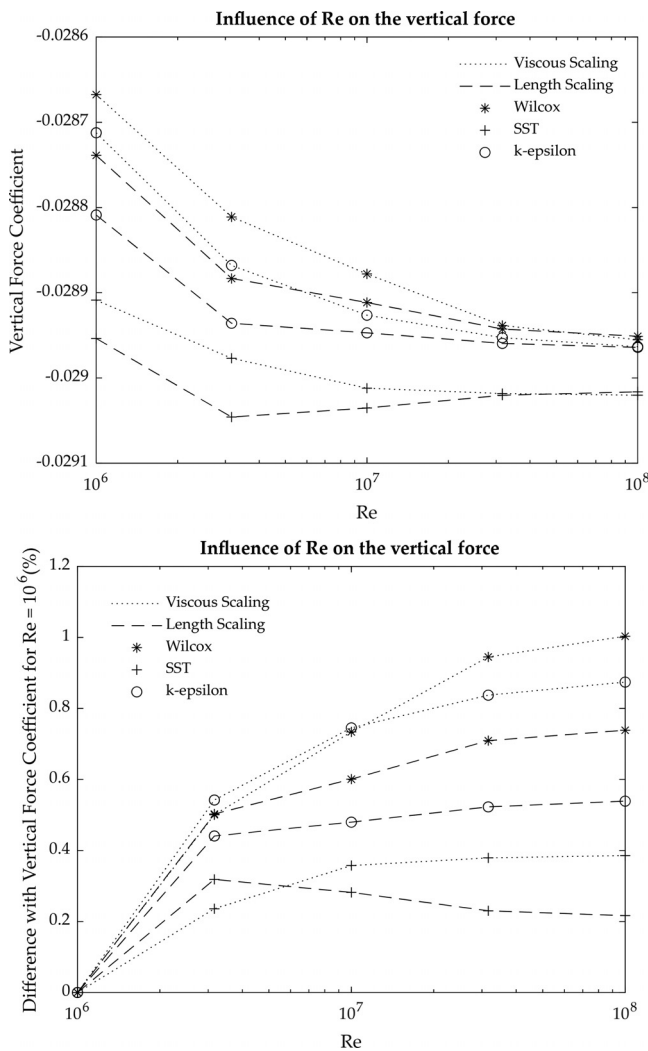

FIG. 5. Scale effects on the vertical force computed with all turbulence models for all Reynolds numbers. Top: variation of the vertical force coefficient with Reynolds number; Bottom: change of the vertical force coefficient relative to the case $Re = 10^6$ (%). Dashed lines show linear length scaling, while dotted lines indicate viscous scaling.
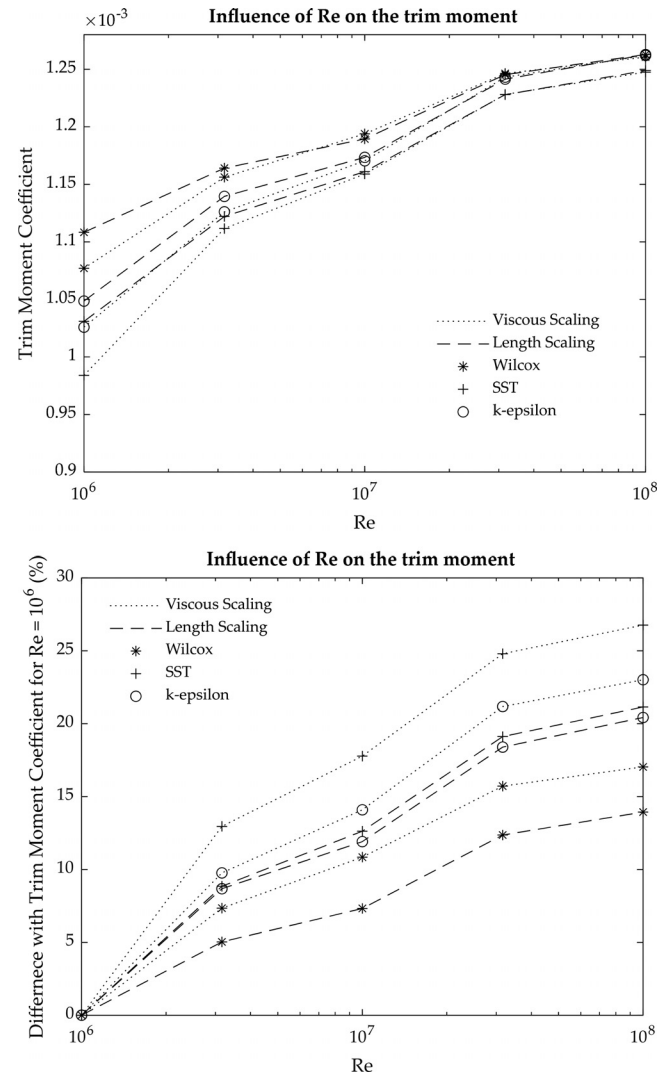

FIG. 6. Scale effects on the trim moment computed with all turbulence models for all Reynolds numbers. Top: variation of the trim moment coefficient with Reynolds number; Bottom: change of the trim moment relative to the case $Re = 10^6$ (%). Dashed lines show linear length scaling, while dotted lines indicate viscous scaling.

predicted when using viscous scaling and employing the SST turbulence model of 26.8%. Conversely, the lowest scale effect is predicted using the k-ω model when length scaling is employed where the scale effect is 13.9%. As was the case for the sinkage, modeling errors are of considerable influence at low Reynolds numbers, showing a maximum deviation of 1.24×10^{-4} or 12.6% of the $k - \omega$ SST model prediction. Nevertheless, all examined turbulence models show the same trend and predict the same order of magnitude of the scale effect. Scale effects are, therefore, more important on the trimming moment than on sinkage, as postulated by Gourlay and Tuck (2001).

The predicted results have significant consequences for trim optimization of ships, which is typically done either using potential flow or at model-scale due to the computational effort involved in accurately resolving full-scale solutions and the lack of engineering standards for high Reynolds number flows. Since neither approach captures the effect of varying boundary layer thickness, the trim moment, therefore trim, at full-scale cannot be reliably predicted using model-scale data. Similarly, experimental studies (Shivachev et al., 2017) of the influence of trim cannot be relied upon to give the exact value of the running trim of a full-scale ship.

Assuming a linear relationship between the trim moment and the trim, the results presented herein show that the full-scale trim of the KCS may vary by as much as 26.8% relative to model-scale. When optimizing the wave resistance of a hull through trim optimization, the scale effect of the trim must, therefore, be accounted for. The results reported herein also confirm the data obtained by Chillcce and Moctar (2022) who modeled the viscous effects on ship squat in shallow water, and Song et al. (2023) who showed large sensitivities of ship trim to roughness—a boundary property affecting chiefly the boundary layer of a hull.

C. Dynamic pressure coefficient distribution on the hull with varying Reynolds number

The Reynolds number dependences of trim moment coefficient and vertical force coefficients imply that a pressure change must be created at the hull surface, as a result of the change in Re. The present section investigates the magnitude of these pressure changes by comparing the dynamic pressure coefficient, C_P, shown in the following equation:

$$C_p = \frac{p - p_{ref}}{0.5\rho_{ref} v_{ref}^2},\tag{9}$$

where $p_{ref} = 0$, v_{ref} is the ship speed and ρ_{ref} is the density of water. To simplify the presentation and interpretation of the data, the integral of the difference in pressure coefficient between $Re = 10^6$ and $Re = 10^8$ over a section is computed. The results for the viscously scaled cases using all turbulence models at $Re = 10^6$ and $Re = 10^8$ are depicted in Fig. 7. Since the differences between Reynolds number are difficult to visualize across the case studies, additional processing was carried out to find the source of the differences between designs. The first step in the analysis was to extract boundary layer extents from the viscously scaled simulations at $Re = 10^6$ and $Re = 10^8$ to investigate the difference in velocity distribution near the aft of the hull, specifically at a distance of L/25 from the aft perpendicular.

As discussed previously, locations near the stern are expected to show the largest differences between scales. Locations near the aft
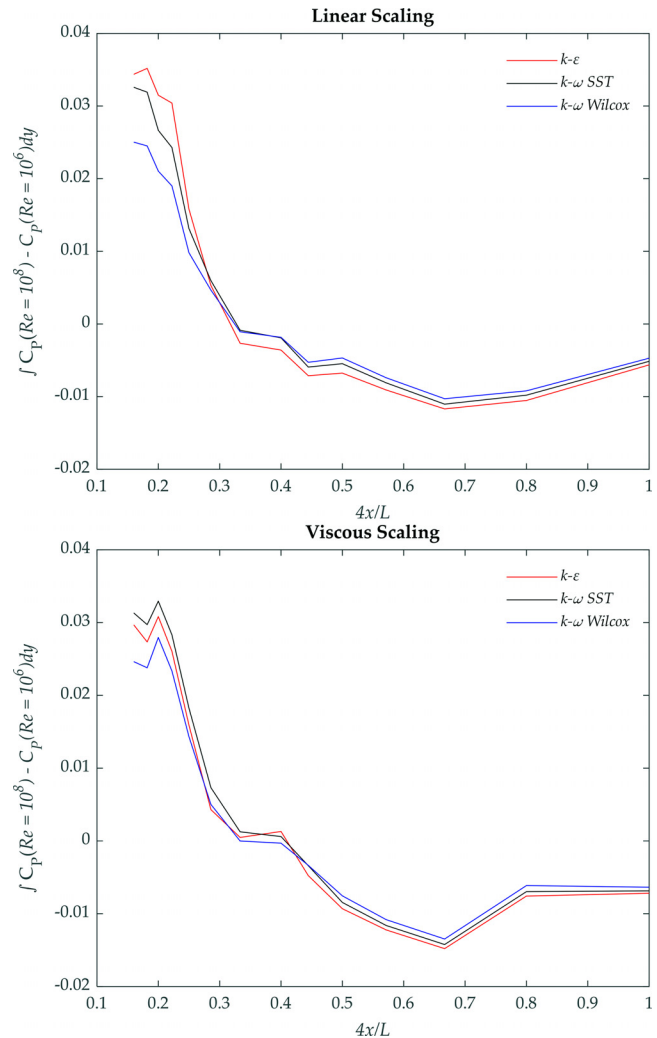

FIG. 7. Integral of the difference of pressure coefficient between $Re = 10^6$ and $Re = 10^8$ for three turbulence models (x = 0 corresponds to the aft perpendicular of the ship and x = 1 to the L/4 section).

perpendicular are, therefore, best suited for the present analysis. The curves depicted in Fig. 8 show the boundary layer extents, measured at locations where the local velocity reaches 90% of the free stream speed at $Re = 10^6$ and $Re = 10^8$ for all turbulence models. The figure shows that minor differences in the velocity distribution obtained with different turbulence models at model scale were compounded and increase at full-scale. In addition, the SST turbulence model predicts a location for the boundary layer extent that falls between the k-ω and k-ε models. To further study how these changes evolve over the aft L/4 section of the ship, the difference in pressure coefficient at varying sections is integrated between $Re = 10^6$ and $Re = 10^8$, as shown in Fig. 7. As discussed earlier and shown in Fig. 8, the differences in boundary layer thickness are expected to accumulate with distance from the bow (Terziev et al., 2021b). These differences affect the pressure distribution, predominantly on the aft
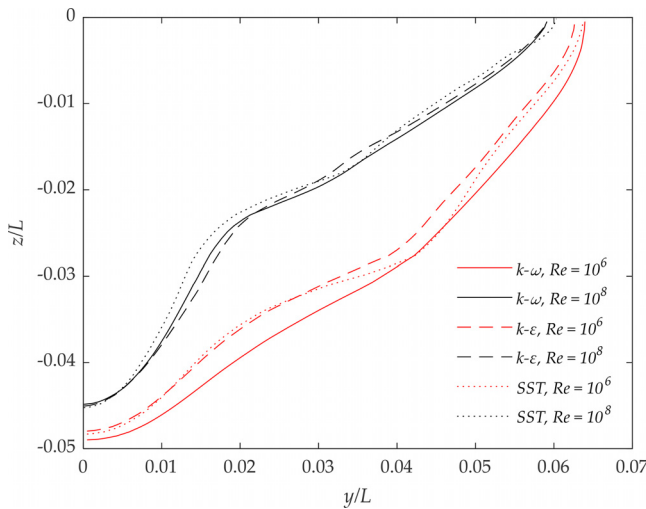
FIG. 8. Boundary layer extents for the viscously scaled simulations using the $k-\omega$, $k-\varepsilon$, and SST turbulence models at $Re = 10^6$ and $Re = 10^8$.

section of the hull, resulting in a varying moment coefficient at different Reynolds numbers.

The results from the integration of the pressure difference at each section between the aft perpendicular and L/4 confirm the cause of the scale effect in the trimming moment with Reynolds number. As the Re grows, the relative thickness of the boundary layer decreases, increasing the velocity closer to the hull. The maximum difference between $Re = 10^6$ and $Re = 10^8$ is 17.32% for L/4, 27.36% for L/6, 48.46% for L/8, and 82.5% for L/10. As can be seen in Fig. 7, the integral of the difference of pressure coefficient rises when with distance from the bow. This explains the changes in trimming moment because when the Reynolds number is higher, the pressure is higher at the aft; hence, the trimming moment will rise. The difference between the integral for $Re = 10^6$ and $Re = 10^8$ is approximately 23.6% to 32.5% at the section L/25 for the different turbulence models, which is the same order of magnitude than the difference for the trim moment.

A source of variation with Reynolds number is the thickness of the boundary layer and its displacement thickness. The overall effect of these variations with Reynolds number results in a different effective underwater shape, which causes the changes in pressure, therefore trimming moment. Such differences are small as demonstrated in Fig. 9; however, they accumulate over the length of the ship with the
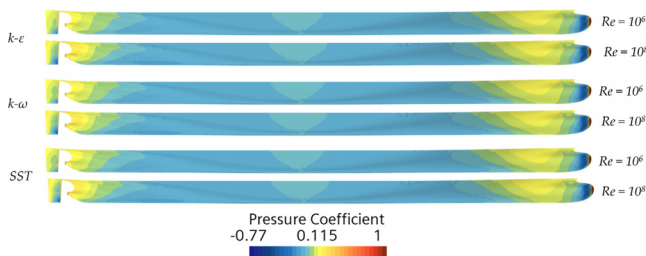
FIG. 9. Dynamic pressure distribution on the surface of the hull.

variation of the boundary layer and result in the deviation between model and full scale shown in Figs. 5 and 6.

D. Form factor

The final set of results to be examined pertain to the form factor using the ITTC and CFD techniques, given in Fig. 10. It should be noted that the ITTC form factor computed from the results of the present numerical model is comparable with prior research. The form factor computed using the ITTC correlation line exhibits the well-known increasing trend with Re. The greatest variation relative to the $Re = 10^6$ k-ε turbulence model of approximately 5.3% when employing viscous scaling. By contrast, the CFD form factor exhibits a reducing trend with increasing Reynolds number. More importantly, the CFD-based form factor shows considerably less variation in magnitude than the ITTC-based form factor of less than 1.37% across all turbulence models. In addition, the sensitivity of the CFD form factor is lesser to modeling errors than the ITTC form factor. In summary, CFD-based form factors show less scale effect and less sensitivity to modeling choices—a key advantage when the impact of modeling errors is difficult to ascertain at full-scale.

There is a risk that re-defining the ITTC-based form factor will lead to loss of generality in extrapolation. As discussed previously, the scale effect on the ITTC-based form factor has been documented extensively as soon as it was proposed, allowing for the development of correction procedures (García-Gómez, 2000; Min and Kang, 2010). Although it could be argued that the ability to correct for scale effects is lost by re-defining the form factor, it is also important to keep in mind that the CFD-based form factor shows considerably less variation and likely requires no Re-based correction. The corrective procedures referred to above can only bring the model-scale form factor closer to the full-scale value but will not eliminate scale effects since they have been developed based on regression rather than the physical mechanism of scale effects.

Returning to the question of Yokoo's (1960) hypothesis, the present results show that even when the ship is kept fixed, the form factor *and* the trimming moment suffer scale effects. Yokoo (1960) asserted that the change in trim causes the form factor variation. It, therefore, seems improbable that these two properties can cancel each other. Instead, boundary layer physics dictates that the thinning of the boundary layer must create cascading differences between the model and the full-scale ship with distance from the bow.

VI. CONCLUSION

The aim of the present study was to identify scale effects of ship trim and sinkage using a RANS approach. Reynolds numbers between 10^6 and 10^8 were modeled by changing the viscosity of water or the length and speed of the ship, keeping a constant Froude number of 0.26, corresponding to the Froude number of the ship in service. The double body method was used to measure the resistance coefficients, the form factor, the trimming moment, and the vertical force acting on the ship. The latter two were used as a surrogate to model scale effects on ship trim and sinkage. In addition, the results were modeled using three turbulence models in order to account for modeling errors within the computational solutions.
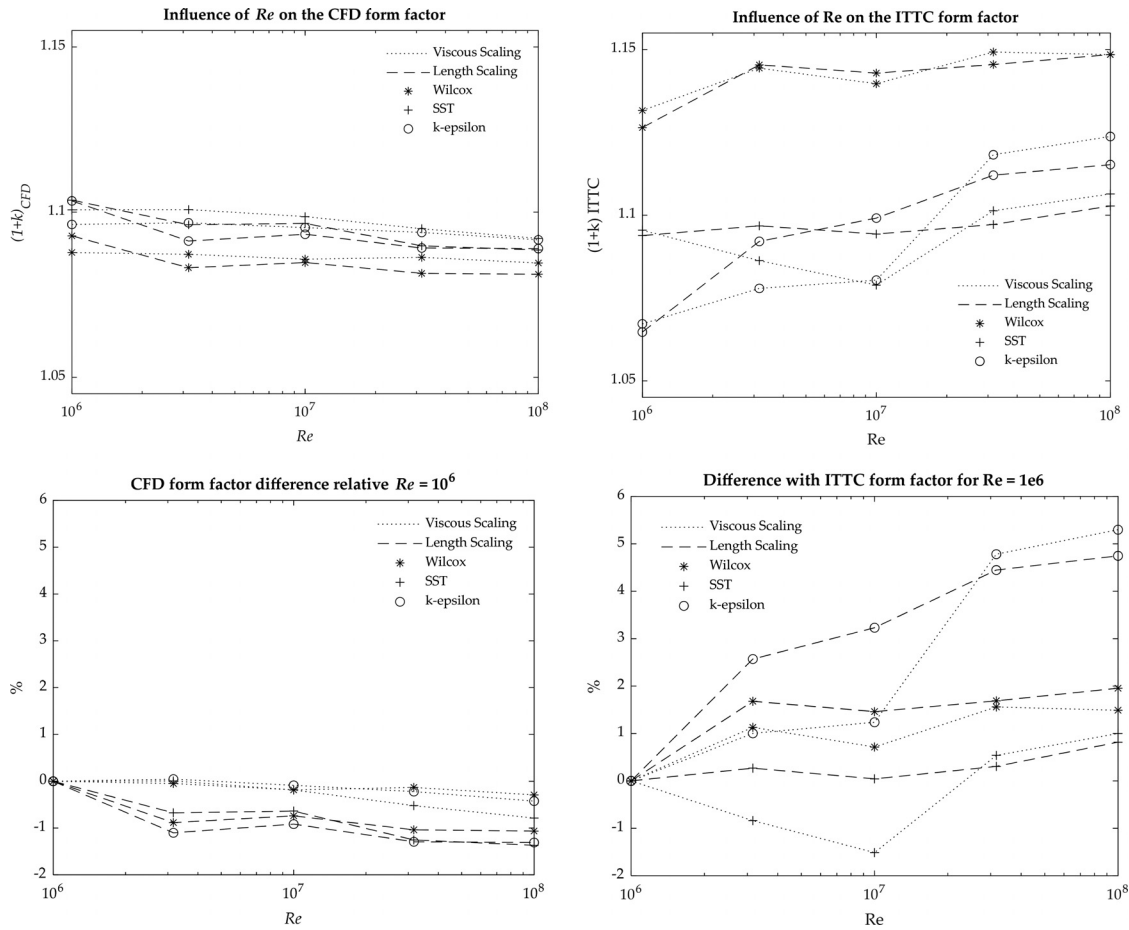
FIG. 10. Scale effects on the form factor. Dashed lines show linear length scaling, while dotted lines indicate viscous scaling.

Results show that scale effects on sinkage can be neglected as the vertical force changes by up to 1%, which was comparable to the discretization uncertainty of the vertical force coefficient of approximately 1.4%. However, the trim is expected to be significantly affected by a change in scale with an increase in 13.9%–26.8% between $Re = 10^6$ and 10^8, depending on the turbulence model. It can, therefore, be concluded that scale effects on the trimming moment are too high to be neglected in trim optimization. Then, trim optimization should be done by simulating at full-scale, notwithstanding the challenges of ensuring robust results in such cases.

The present research could be extended in a variety of ways, but a key consequence arising from the conclusions drawn herein relates to the magnitude of the overall total resistance and its composition. Specifically, since friction takes a dominant role in most commercial ships that travel at relatively low speeds, can wave-resistance-based trim optimization deteriorate overall performance by increasing the form factor? Or alternatively, can trim optimization be re-framed for slow merchant craft in terms of the form factor rather than just the wave resistance and is it possible to optimize both, simultaneously? Finally, a piece of work under way relates to the modeling of the form factor of unevenly trimmed ships and how that changes the balance of the total resistance makeup.

In conducting the present study, priority was given to scale effects at a single speed. While it is known that the Froude number does not influence significantly the form factor beyond very low speeds, it is worthwhile to test the magnitude of the scale effect on the trim and sinkage and lower Froude numbers. Trim follows a complicated pattern with increases in Froude number, which cannot be captured by the double body method used herein, warranting further study by methods that capture the free surface and motion of the ship.

ACKNOWLEDGMENTS

AUTHOR DECLARATIONS
Conflict of Interest

The authors have no conflicts to disclose.

Author Contributions

Maxime Le Strat: Conceptualization (supporting); Data curation (lead); Formal analysis (lead); Investigation (lead); Methodology (equal); Resources (supporting); Software (lead); Validation (equal); Visualization (equal); Writing – original draft (lead); Writing – review & editing (lead). **Momchil Terziev:** Conceptualization (lead); Data curation (supporting); Investigation (supporting); Methodology (equal); Project administration (lead); Resources (lead); Software (lead); Supervision (lead); Validation (equal); Visualization (equal); Writing – original draft (supporting); Writing – review & editing (supporting).

DATA AVAILABILITY

The data that support the findings of this study are available from the corresponding author upon reasonable request.

REFERENCES

ASME (American Society of Mechanical Engineers), "Standard for verification and validation in computational fluid dynamics and heat transfer - ASME V&V 20–2009," in *ASME International* (ASME, 2009).

Beck, R. F., Newman, J. N., and Tuck, E. O., "Hydrodynamic forces on ships in dredged channels," J. Ship Res. **19**(3), 166–171 (1975).

Chillcce, G., and Moctar, O., "Viscous effects on squat," Appl. Ocean Res. **125**, 103252 (2022).

Eca, L., Vaz, G., and Hoekstra, M., "Iterative errors in unsteady flow simulations: Are they really negligible?," in *20th Numerical Towing Tank Symposium (NuTTS-2017)* (Numerical Towing Tank Symposium, 2017), pp. 1–5.

Elsherbiny, K., Tezdogan, T., Kotb, M., Incecik, A., and Day, S., "Experimental analysis of the squat of ships advancing through the New Suez Canal," Ocean Eng. **178**, 331–344 (2019).

Ferguson, A. M., *Factors Affecting the Components of Ship Resistance* (University of Glasgow, 1977).

García-Gómez, A., "On the form factor scale effect," Ocean Eng. **27**(1), 97–109 (2000).

Gourlay, T., "Ship squat in water of varying depth," IJME **145**(a1), 12 (2003).

Gourlay, T. P., and Tuck, E. O., "The maximum sinkage of a ship," J. Ship Res. **45**(1), 50 (2001).

Haase, M., Zurcher, K., Davidson, G., Binns, J. R., Thomas, G., and Bose, N., "Novel CFD-based full-scale resistance prediction for large medium-speed catamarans," Ocean Eng. **111**, 198–208 (2016).

ITTC, "Uncertainty analysis in CFD verification and validation methodology and procedures," in 25th ITTC 2008, Resistance Committee (ITTC, 2008), Vol. 12.

ITTC, "Recommended procedures 1978 ITTC performance prediction method, 4th revision, 7.5 – 02 03 – 01.4," in *28th International Towing Tank Conference* (ITTC, 2017).

Kim, W. J., Van, S. H., and Kim, D. H., "Measurement of flows around modern commercial ship models," Exp. Fluids **31**(5), 567–578 (2001).

Kok, Z., Duffy, J., Chai, S., Jin, Y., and Javanmardi, M., "Numerical investigation of scale effect in self-propelled container ship squat," Appl. Ocean Res. **99**, 102143 (2020).

Korkmaz, K. B., Werner, S., and Bensow, R., "Verification and validation of CFD based form factors as a combined CFD/EFD method," JMSE **9**(1), 75–30 (2021).

Korkmaz, K. B., Werner, S., and Bensow, R., "Numerical friction lines for CFD based form factor determination method," in *MARINE VIII: Proceedings of the VIII International Conference on Computational Methods in Marine Engineering* (CIMNE, 2019).

Korkmaz, K. B., Werner, S., Sakamoto, N., Queutey, P., Deng, G., Yuling, G., Guoxiang, D., Maki, K., Ye, H., Akinturk, A., Sayeed, T., Hino, T., Zhao, F., Tezdogan, T., Demirel, Y. K., and Bensow, R., "CFD based form factor determination method," Ocean Eng. **220**, 108451 (2021).

Menter, F. R., "Two-equation eddy-viscosity turbulence models for engineering applications," AIAA J. **32**(8), 1598–1605 (1994).

Min, K. S., and Kang, S. H., "Study on the form factor and full-scale ship resistance prediction method," J. Mar. Sci. Technol. **15**(2), 108–118 (2010).

Ponkratov, D., "Working together for a safer world," in *Proceedings 2016 Workshop on Ship Scale Hydrodynamic Computer Simulation* (Lloyd's Register, 2017).

Richardson, L. F., "IX. The approximate arithmetical solution by finite differences of physical problems involving differential equations, with an application to the stresses in a masonry dam," Philos. Trans. R. Soc. London, Ser. A **210**(459–470), 307–357 (1911).

Richardson, L. F., and Arthur Gaunt, J., "VIII. The deferred approach to the limit," Philos. Trans. R. Soc. London, Ser. A **226**(636–646), 299–361 (1927).

Roache, P. J., "Quantification of uncertainty in computational fluid dynamics," Annu. Rev. Fluid Mech. **29**(1), 123–160 (1997).

Roache, P. J., Ghia, K. N., and White, F., "Editorial policy statement on the control of numerical accuracy," J. Fluids Eng. **108**, 2 (1986).

Salas, M. D., "Some observations on grid convergence," Comput. Fluids **35**(7), 688–692 (2006).

Shivachev, E., Khorasanchi, M., and Day, A. H., "Trim influence on KRISO container ship (KCS); an experimental and numerical study," in *Proceedings of the ASME 2017 36th International Conference on Ocean, Offshore and Arctic Engineering* (ASME, 2017), pp. 1–7.

Song, S., Terziev, M., Tezdogan, T., Demirel, Y. K., De Marco Muscat-Fenech, C., and Incecik, A., "Investigating roughness effects on ship resistance in shallow waters," Ocean Eng. **270**, 113643 (2023).

Terziev, M., Tezdogan, T., Demirel, Y. K., Villa, D., Mizzi, S., and Incecik, A., "Exploring the effects of speed and scale on a ship's form factor using CFD," Int. J. Naval Archit. Ocean Eng. **13**, 147–162 (2021a).

Terziev, M., Tezdogan, T., and Incecik, A., "A geosim analysis of ship resistance decomposition and scale effects with the aid of CFD," Appl. Ocean Res. **92**, 101930 (2019).

Terziev, M., Tezdogan, T., and Incecik, A., "Application of eddy-viscosity turbulence models to problems in ship hydrodynamics," Ships Offshore Struct. **15**(5), 511–534 (2020).

Terziev, M., Tezdogan, T., and Incecik, A., "A numerical assessment of the scale effects of a ship advancing through restricted waters," Ocean Eng. **229**, 108972 (2021b).

Terziev, M., Tezdogan, T., and Incecik, A., "Scale effects and full-scale ship hydrodynamics: A review," Ocean Eng. **245**, 110496 (2022).

Tuck, E. O., "Shallow-water flows past slender bodies," J. Fluid Mech. **26**(1966), 81–95 (1966).

Tuck, E. O., "Sinkage and trim in shallow water of finite width," Schiffstechnik **14**(73), 92–94 (1967).

Wang, J. B., Yu, H., and Feng, Y., "Feasible study on full-scale delivered power prediction using CFD/EFD combination method," J. Hydrodyn. **31**(6), 1250–1254 (2019).

Wilcox, D. C., "Formulation of the kw turbulence model revisited," AIAA J. **46**(11), 2823–2838 (2008).

Xing, T., and Stern, F., "Factors of safety for Richardson extrapolation," J. Fluids Eng. **132**(6), 061403 (2010).

Yokoo, K., "Effect of sinkage and trim on form factor of resistance," J. Zosen Kiokai **1960**, 15–22 (1960).